

## NONTHERMAL $\gamma$ /X-RAY FLASHES FROM SHOCK BREAKOUT IN GAMMA-RAY BURSTS/SUPERNOVAE

XIANG-YU WANG<sup>1,2</sup>, ZHUO LI<sup>3</sup>, ELI WAXMAN<sup>3</sup> AND PETER MÉSZÁROS<sup>1,4</sup>

*Draft version September 12, 2018*

### ABSTRACT

Thermal X-ray emission which is simultaneous with the prompt gamma-rays has been detected for the first time from a supernova connected with a gamma-ray burst (GRB), namely GRB060218/SN2006aj. It has been interpreted as arising from the breakout of a mildly relativistic, radiation-dominated shock from a dense stellar wind surrounding the progenitor star. There is also evidence for the presence of a mildly relativistic ejecta in GRB980425/SN1998bw, based on its X-ray and radio afterglow. Here we study the process of repeated bulk Compton scatterings of shock breakout thermal photons by the mildly relativistic ejecta. During the shock breakout process, a fraction of the thermal photons would be repeatedly scattered between the pre-shock material and the shocked material as well as the mildly relativistic ejecta and, as a result, the thermal photons get boosted to increasingly higher energies. This bulk motion Comptonization mechanism will produce nonthermal gamma-ray and X-ray flashes, which could account for the prompt gamma-ray burst emission in low-luminosity supernova-connected GRBs, such as GRB060218. A Monte Carlo code has been developed to simulate this repeated scattering process, which confirms that a significant fraction of the thermal photons get “accelerated” to form a nonthermal component, with a dominant luminosity. This interpretation for the prompt nonthermal emission of GRB060218 may imply that either the usual internal shock emission from highly relativistic jets in these low-luminosity GRBs is weak, or alternatively, that there are no highly relativistic jets in this peculiar class of bursts.

*Subject headings:* gamma rays: bursts — supernovae: general — shock waves

### 1. INTRODUCTION

Supernova shock breakout has been predicted for a few decades (e.g. Colgate 1974; Klein & Chevalier 1978; Ensmann & Burrows 1992; Blinnikov et al. 1998, Matzner & McKee 1999). In core collapse supernovae, a shock wave is generated which propagates through the progenitor star and ejects the envelope. As the shock propagates through the envelope, it is mediated by radiation: The post shock energy density is dominated by radiation, and the shock transition is mediated by Compton scattering. As the shock approaches the edge of the star, the optical depth of the plasma lying ahead of the shock decreases. At the radius where the optical depth drops to  $\sim c/v_s$ , where  $v_s$  is the shock velocity, Compton scattering can no longer sustain the shock, and the shock undergoes a transition to a viscous shock (or a collisionless shock, Waxman & Loeb 2001). This transition is accompanied by a bright ultraviolet/X-ray burst, as photons escape far ahead of the shock due to the low optical depth. The term “shock breakout” is commonly used to refer to the emergence of the shock from the edge of the star. However, if the star is surrounded by an optically thick wind, the radiation mediated shock would continue to propagate into the wind, up to the point where the wind optical depth drops below  $\sim c/v_s$ . In this case, shock breakout, i.e. the transition from a radiation mediated shock to a viscous (or collisionless) one accompanied by a bright ultraviolet/X-ray burst, occurs as the shock propagates through the wind, at a radius which may be significantly larger than the star’s radius. We use here the term “shock breakout” to denote this transition in general, regard-

less of whether it occurs as the shock reaches the edge of the star or further out within an optically thick wind.

Shock breakout has previously never been directly detected from any supernovae due to its transient nature and its very early (minutes to hours) occurrence, in the absence of a suitably prompt trigger alert. Recently, thanks to its sensitive gamma-ray trigger and rapid slewing capability, *Swift* has detected early thermal X-rays emission from a supernova associated with a GRB, namely GRB060218/SN2006aj (e.g. Campana et al. 2006; Pian et al. 2006; Mazzali et al. 2006; Modjaz et al. 2006; Sollerman et al. 2006; Mirabel et al. 2006; Cobb et al. 2006; Soderberg et al. 2006; Liang et al. 2006a), which has been interpreted as arising from the breakout of a radiation-dominated shock (Campana et al. 2006; Waxman et al. 2007).

The large energy carried by thermal X-rays,  $\sim 10^{49}$  erg, and the long duration ( $\sim 1000$  s) of the thermal X-ray emission implies that shock breakout must occur at a radius of  $\sim 10^{13}$  cm. The lack of Hydrogen lines implies, on the other hand, a compact progenitor, a WR star of radius  $\sim 10^{11}$  cm. This suggests that the progenitor was surrounded by an optically thick wind, and that shock breakout occurred at a radius  $\sim 10^{13}$  cm, where the optical depth of the wind becomes small enough. The inferred mass loss rate,  $\sim 3 \times 10^{-4} M_{\odot}/\text{yr}$  (Campana et al. 2006) is consistent with that typically expected for WR stars (e.g. Felli & Panagia 1982; Nugis & Lamers 2000, 2002)<sup>5</sup>. Another possibility is that the shock breaks out from an optically thick shell pre-ejected from the progenitor (the required shell mass is only  $10^{-7} M_{\odot}$ , see Campana et al.

<sup>1</sup> Department of Astronomy and Astrophysics, Pennsylvania State University, University Park, PA 16802, USA

<sup>2</sup> Department of Astronomy, Nanjing University, Nanjing 210093, China

<sup>3</sup> Physics Faculty, Weizmann Institute of Science, Rehovot 76100, Israel

<sup>4</sup> Department of Physics, Pennsylvania State University, University Park, PA 16802, USA

<sup>5</sup> The arguments based on radio observations against the presence of an optically thick wind (Fan et al. 2006), are not conclusive, since radio observations do not allow one to determine the explosion parameters. In particular, the estimates for the kinetic energy range between  $\sim 10^{48}$  erg and  $\sim 10^{50}$  erg, and the ambient medium density estimates range between  $\sim 10^0 \text{cm}^{-3}$  and  $\sim 10^2 \text{cm}^{-3}$  (Soderberg et al. 2006; Fan et al. 2006).

2006).

The simple result, that a wind photospheric radius  $R_{ph} \sim 10^{13}$  cm is required to account for the thermal emission as due to shock break out from a wind, is supported by the calculations of Li (2007), who finds that the radius at which the wind optical depth equals 20 is required to be  $R_* \sim 100R_\odot$ . Since the wind models investigated in Li (2007) have  $1.5 \lesssim R_{ph}/R_* < 3$  (compare his figures 12 and 3), his conclusion implies that  $R_{ph} \sim 10^{13}$  cm is required, consistent with our conclusion. Note, however, that the claim that  $R_* \sim 100R_\odot$  is required is not robust, since the ratio  $R_{ph}/R_*$  depends on the adopted wind velocity profile, and is likely to be  $> 3$  for WR stars. Note also that when the mass loss is well above  $10^{-4}M_\odot\text{yr}^{-1}$ , the wind becomes very optically thick and the apparent stellar radius grows, so that the star no longer looks like a WR star (Nino Panagia, personal communication). It should also be pointed out that the analysis of the required wind properties in Li (2007) is far too restricted. A model is adopted by Li (2007) where the shock is produced by a spherical explosion with fixed energy ( $2 \times 10^{51}$  erg) and fixed ejecta mass ( $2M_\odot$ ), and its acceleration is due to propagation through the model wind profile. Beyond the fact that dependence on the explosion parameters is not explored, it is not at all clear that this is the correct description of shock dynamics. In fact, it is known that such shock acceleration models (Matzner & McKee 1999; Tan et al. 2001) can not account for the energy deposited in the mildly relativistic ejecta,  $v/c=0.8$ , observed in GRB 980425/SN1998bw (Kulkarni et al. 1998, Waxman & Loeb 1999, Chevalier & Li 1999, Waxman 2004). It could be, e.g., that this mildly-relativistic shock is driven instead by a choked jet propagating through the progenitor.

From the thermal energy density of the shock, Campana et al. (2006) have inferred that the shell driving the radiation-dominated shock in GRB060218/SN2006aj must be mildly relativistic, with a velocity  $\Gamma\beta \sim 1-2$ , where  $\beta$  is the velocity in units of the speed of light  $c$  and  $\Gamma = (1 - \beta^2)^{-1/2}$  is the Lorentz factor. This shock could be driven by the outermost parts of the envelope that get accelerated to a mildly relativistic velocity when the supernova shock accelerates in the density gradient of the envelope of the supernova progenitor (Colgate 1974; Matzner & McKee 1999; Tan et al. 2001), probably a Wolf-Rayet (WR) star. The more compact configuration of a WR star, compared with a blue or red supergiant, and the large explosion energy characterizing a hypernovae may help to accelerate a considerable amount of matter to a mildly relativistic, and probably anisotropic velocity distribution (see however the comment above on SN1998bw).

Due to the connection with a GRB, there are also other possibilities for the origin of this radiation-dominated shock. In the collapsar model for GRBs, the shock could be driven by the cocoon of a relativistic jet (Mészáros & Rees 2001; Ramirez-Ruiz et al. 2002; Zhang et al. 2003) or the slower ( $\Gamma\beta \sim 1-2$ ), high-latitude outer parts of a relativistic jet. The emergence of the shock in this case would be highly non-spherical. As pointed out in Campana et al. (2006), observations require a non-spherical shock breakout. This does not necessarily imply a shock driven by a cocoon/jet, since the wind itself may be highly non-spherical<sup>6</sup>. Observations of high optical polarization in SNe at early times of 3-5 days

<sup>6</sup> We note in this context that the claim in Ghisellini et al. (2006b), that the optical emission and the thermal X-ray emission are not due to the same thermal component is not necessarily valid, since Ghisellini et al. (2006b) assume spherical symmetry and neglect in addition light travel time effects.

(e.g. Gorosabel et al. 2006) are also consistent with non-spherical shocks.

The relatively flat light curve of the X-ray afterglow of the nearest GRB, GRB980425/SN1998bw, up to  $\sim 100$  days after the burst, has been argued to be caused by the coasting phase of a mildly relativistic shell with energy of a few times  $10^{49}$ erg (Waxman 2004). Similarly, the X-ray afterglow of another nearby GRB, GRB031203/SN2003lw also had an early flat light curve (Watson et al. 2004). Thus, it is possible that a mildly relativistic ejecta is ubiquitous in supernovae-associated GRBs. In this paper, we suggest that the non-thermal X-ray and gamma-ray emission in such objects can arise from repeated bulk-Compton scatterings (i.e. bulk motion Comptonization) of thermal shock breakout X-rays photons.

Blandford & Payne (1981) first noted the importance of bulk motion acceleration of photons in a radiation-dominated shock. They found that photons are preferentially upscattered by the bulk motion rather than by the thermal motions of the electrons, and a power-law spectrum extending to high energies forms, when the electron thermal velocity is less than the shock velocity  $v_s$ . Repeated scatterings using the energy of the bulk motions of two approaching relativistic shells in the context of GRB internal shocks was studied by Gruzinov & Mészáros (2000). They found that the seed synchrotron photons can be boosted to much higher energies, which is confirmed by their Monte Carlo simulations. This process is equivalent to the Fermi acceleration mechanism of particles (Blandford & Eichler 1987) or photon scattering off Alfvén waves (Thompson 1994), but here the mechanism, instead, uses the relative bulk motion and accelerates photons. The bulk motion Comptonization mechanism has also been invoked to interpret the high-energy spectra of accreting black holes (e.g. Shrader & Titarchuk 1998; Titarchuk & Shrader 2005).

## 2. THE BULK MOTION COMPTONIZATION MODEL

Consider a mildly relativistic ejecta driving a radiation-dominated shock into the stellar envelope of the GRB/SN progenitor or into an optically thick wind (or pre-ejected shell) surrounding it. Once the optical depth of the material in front of the shock drops below  $c/v_s$  (where  $v_s$  is the shock velocity), the photons escape and produce a breakout flash. Since the Thompson scattering optical depth is non-negligible in front of the shock while the shock is breaking out, some fraction of the thermal photons will be scattered back. The back-scattered photons will be scattered forward by the expanding ejecta or shocked plasma, boosting up their energy. The backward-forward scattering cycle may repeat itself many times for some fraction of the photons, boosting their energy by a large factor.

For GRB060218/SN2006aj, the shock breakout may occur in the wind or a pre-ejected shell, which serves as the scattering medium target. The radius where a mildly relativistic radiation-dominated shock breaks out from a dense wind is

$$R_{br} \simeq 2 \times 10^{12} \text{cm} \left( \frac{\dot{M}}{10^{-4}M_\odot\text{yr}^{-1}} \right) \left( \frac{v_w}{10^8 \text{cm s}^{-1}} \right)^{-1}, \quad (1)$$

where  $\dot{M}$  is the mass loss rate and  $v_w$  is the wind velocity. The optical depth of the ejecta itself at the shock breakout radius is

$$\tau_{ej} = \frac{\sigma_T E_k}{4\pi(\Gamma-1)m_p c^2 R^2} = 35 E_{k,50} \left( \frac{R_{br}}{10^{13} \text{cm}} \right)^{-2} (\Gamma-1)^{-1}, \quad (2)$$

where  $E_k = 10^{50} E_{k,50}$  erg is the (isotropic equivalent) kinetic energy of the mildly relativistic shell. For  $E_{k,50} \sim 1$ ,  $\tau_{ej}$  is much larger than unity, and the ejecta can be regarded as a mirror which effectively reflects all the photons incident upon it.

The post-shock electron temperature is determined by the balance between heating by the ion-electron collisions and Compton cooling by the thermal shock breakout photons. For a shock velocity  $v_s$ , the ion temperature is  $kT_i = (3/16)\mu v_s^2 \simeq 9 \times 10^7 (v_s/c)^2$  eV, where  $\mu = m_p/2$  is the mean atomic mass per particle for a plasma in which the thermal energy is shared equally between protons and electrons (Waxman & Loeb 2001). The ion-electron collision rate is  $\nu_{ie} = 2 \times 10^{-2} (\rho/10^{-11} \text{gcm}^{-3}) (kT_i/10^8 \text{eV})^{-3/2} \text{s}^{-1}$  for  $T_e < m_e T_i/m_p$  (e.g. Krall & Trivelpiece 1973), while the Compton scattering cooling rate is  $\nu_{\text{Comp}} = (8\sigma_T/3m_e c) a T_{th}^4 = 5000 (kT_{th}/0.15 \text{KeV})^4 \text{s}^{-1}$ , where  $\rho \simeq 4\rho_w = 2 \times 10^{-11} (\dot{M}/10^{-4} M_\odot \text{yr}^{-1}) (v_w/10^8 \text{cms}^{-1})^{-1} R_{\text{br},12}^2 \text{g cm}^{-3}$  is the mass density of the shocked wind,  $\rho_w$  is the density of the pre-shocked wind and  $T_{th}$  is the temperature of the thermal photons. The electron temperature is determined by the balance between heating and cooling  $\nu_{ie} T_i = \nu_{\text{Comp}} T_e$ , which gives

$$kT_e \sim 0.3 \left(\frac{v_s}{c}\right) \left(\frac{\rho}{10^{-11} \text{gcm}^{-3}}\right) \left(\frac{k_B T_{th}}{0.15 \text{KeV}}\right)^{-4} \text{KeV}. \quad (3)$$

Thus, the electrons can be regarded as being essentially cold, in comparison with the mildly relativistic bulk motion.

Below we first present in § 2.1 a qualitative description of the bulk Comptonization emission, by analogy to the Comptonization mechanism in thermal electron plasma. This description is based on results obtained assuming a fixed optical depth  $\tau$  for the scattering medium in front of the shock. In reality, the optical depth is decreasing with time due to shock expansion, and may therefore change considerably between repeated photon scattering. In fact, the time scale for a single scattering cycle is typically comparable to the shock expansion time, and only a small fraction of the photons are scattered on a shorter time scale and gain considerable energy. In § 2.2 we present a discussion based on a one-dimension Monte Carlo simulation of this process, which takes into account the time dependence of the optical depth. The purpose of this simulation is to give a qualitative analysis of the shock breakout bulk Comptonization mechanism, and to explore whether the non-thermal component can be indeed dominant. A detailed, full three-dimension Monte-Carlo simulation would require a full understanding of the shock structure and the anisotropic geometry (as discussed in § 2.2 in more detail), which is, however, largely unknown at present. In § 2.3 we discuss the implications to GRB060218/SN2006aj.

### 2.1. A qualitative description

Ignoring the time dependence of  $\tau$ , the optical depth ahead of the shock, the physical situation is similar to that of Comptonization by a thermal electron plasma. In the present case, the electrons are cold and their momentum is dominated by the bulk motion. Multiple scattering in a thermal electron plasma can lead to a power-law spectrum of the scattered photons (Pozdnyakov et al. 1976; 1983), which has found application in many astrophysical contexts. Dermer, Liang & Canfield (1991) further extended this to a mildly relativistic thermal plasma. Assuming each scattering amplifies the photon energy by a factor  $A$ , the energy of a photon escaping after

$k$  scatterings is  $\varepsilon_k = \varepsilon_i A^k$ , where  $\varepsilon_i$  and  $\varepsilon_k$  are the initial and final photon energies respectively. For fixed  $\tau$ , a photon scattered by the ejecta has a probability  $1 - e^{-\tau}$  to be scattered back towards the ejecta, and a probability  $e^{-\tau}$  to escape. The probability for a photon to undergo  $k$  scatterings before escaping is  $(1 - e^{-\tau})^k$ , and since the photon energy is multiplied by  $A$  per scattering, the escaping photon intensity would have a power-law shape

$$F(\varepsilon_k) \sim F(\varepsilon_i) (1 - e^{-\tau})^k \sim F(\varepsilon_i) (\varepsilon_k/\varepsilon_i)^{-\alpha} \quad (4)$$

with

$$\alpha = -\ln(1 - e^{-\tau})/\ln A. \quad (5)$$

The photon energy amplification factor  $A$  is determined by the kinetic energy of the electrons. For trans-relativistic electrons and isotropic photon distributions,  $A \sim \Gamma^2(1 + \beta^2/3)$ . The power-law spectrum extends to a cutoff energy, which is the smaller of the electron kinetic energy,  $\sim (\Gamma - 1)m_e c^2$ , and its rest mass  $m_e c^2$  (due to the Klein-Nishina effect).

An important difference between the usual thermal electron (or bulk) Comptonization case and the current case is that in the present case the scattering optical depth decreases with time as the mildly relativistic ejecta moves outward. Initially, when the optical depth  $\tau \gtrsim 1$ , the slope of  $\nu F_\nu$  is positive and most radiation is emitted at high energies. As  $\tau$  decreases, the spectrum becomes softer and softer, and at late times the spectrum is composed of a thermal peak plus a weak high-energy power-law tail. In general, we expect a noticeable spectral softening of the nonthermal emission with time. This spectral softening is expected to be accompanied by a decrease in the Compton luminosity. At early time, when the effective Compton parameter  $Y = A(1 - e^{-\tau}) > 1$ , the Compton luminosity may exceed the thermal luminosity (it is limited by the kinetic energy of the ejecta  $E_k$ ). We expect the Compton luminosity to decrease with time, as  $Y$  decreases.

The gamma-ray light curves produced in this model generally have a simple profile without multi-peak structure. The characteristic variability timescale  $\delta t$  of the burst is determined by the radius  $R$  where the optical depth of the material ahead of the shock drops to  $\sim 1$ , i.e.  $\delta t \sim R(\tau = 1)/c$  (If the stellar wind surrounding the progenitor were optically thin everywhere, the shock would break out from the SN progenitor stellar envelope and the variability time would be about  $R_*/c$ , where  $R_*$  is the stellar radius.)

### 2.2. Monte Carlo simulation of photon “acceleration”

As the shock propagates outward, the optical depth  $\tau$  ahead of the shock decreases with time. In order to understand the photon “acceleration” mechanism in this time-dependent case, we carried out a Monte Carlo simulation of repeated Compton scattering during shock breakout from a dense stellar wind. We approximate the hydrodynamics of the problem as follows. We consider the mildly relativistic ejected shell to act as a piston with a time-independent bulk Lorentz factor  $\Gamma$  and an infinite optical depth  $\tau_{ej}$ . Since the stellar wind swept up by the ejecta is not sufficient to decelerate it, the constant velocity of the interface is justified. This “piston” drives a shock into the surrounding medium, where the density profile is assumed to follow  $n \propto R^{-2}$ . We assume the shock width to be infinitesimal. There are three distinct regions in this picture: The moving piston, the shocked medium and the pre-shocked medium. The shocked medium is considered to form a homogeneous shell, and the electrons are regarded as cold,

as follows from Eq. (3), with a bulk velocity same as that of the ejecta. The velocity of the shock front can then be obtained consistently from the shock jump condition. We further simplify the problem by considering a one-dimensional situation, where the motion of the photons is confined to one dimension, forward or backward relative to the shock expansion direction. The photons are injected at the shock front and would then be repeatedly scattered among these three components until they escape out to a sufficiently further region. Our simulation takes into account the proper possibility of photon scattering by each of the three components (with the appropriate photon energy gain or loss). The photon scattering probability by the unshocked wind and shocked wind is determined by the optical depth of each component, while the piston is regarded as a mirror since it has a larger optical depth much larger than unity.

We note here that this level of simplification (i.e. the one-dimensional treatment) is appropriate for the uncertainties inherent in such a scenario. Aside from the geometrical uncertainties associated with the non-spherical scenario, discussed further below, even in a spherical approximation a complete calculation of the light curve and spectrum of escaping photons would require a detailed calculation of the shock structure, including the back-reaction of “accelerated” photons on the shock-the angular and energy distribution of electrons and photons across the shock transition, which would determine the distribution of “photon injection times” and the distribution of electron Lorentz factors across the shock. In order to do this, it would not be sufficient to carry out a 3-D Monte Carlo calculation of the Comptonization, where the photons are treated as test particles. Rather, the structure of the shock and the radiation field would need to be solved self-consistently, since the radiation field affects the shock structure (electron energy distribution etc). While such solutions exist for non relativistic shocks (Weaver 1976), the structure of radiation-dominated shocks is not known even for mildly relativistic shocks ( $v/c > 0.1$ ). Constructing such a self-consistent solution would be beyond the scope of the present manuscript.

We study the spectra of escaping photons, which result from the “injection” of photons at the shock front at various radii, corresponding to various values of  $\tau$  at the injection time, denoted by  $\tau_{\text{inj}}$ . The photons are treated as “test particles”, and their scattering history is followed as the shock expands and  $\tau$  decreases. The resulting time-integrated  $\nu F_\nu$  spectra are given in Fig. 1 for two values of  $\Gamma$ ,  $\Gamma = 2$  and  $\Gamma = 1.5$ . The red, blue, olive and black curves describe the spectrum of escaping photons resulting from the injection of a thermal distribution of photons at  $\tau_{\text{inj}} = 2, c/v_s, 0.5$  and  $0.2$  respectively. The injected photons are assumed to have a thermal spectrum with  $T = 0.15$  keV. The “humps” seen in the simulated spectra correspond to different orders of Compton scattering, with two nearby humps separated by  $\sim \Gamma^2$ . These humps appear because we do not consider in our one-dimensional simulation the angular distribution of scattered photons. In reality, these humps are expected to be smoothed out. Fig. 1 demonstrates that a significant fraction the thermal photons that are injected at optical depth  $\tau_{\text{inj}} \sim 1$ , where the photons are expected to escape the shock, may be “accelerated” to high energy. The resulting non-thermal component may carry a significant fraction of the shell energy, and its luminosity may exceed that of the thermal component. As expected, the spectrum depends on  $\Gamma$  and on  $\tau_{\text{inj}}$ , with harder spectra obtained for larger val-

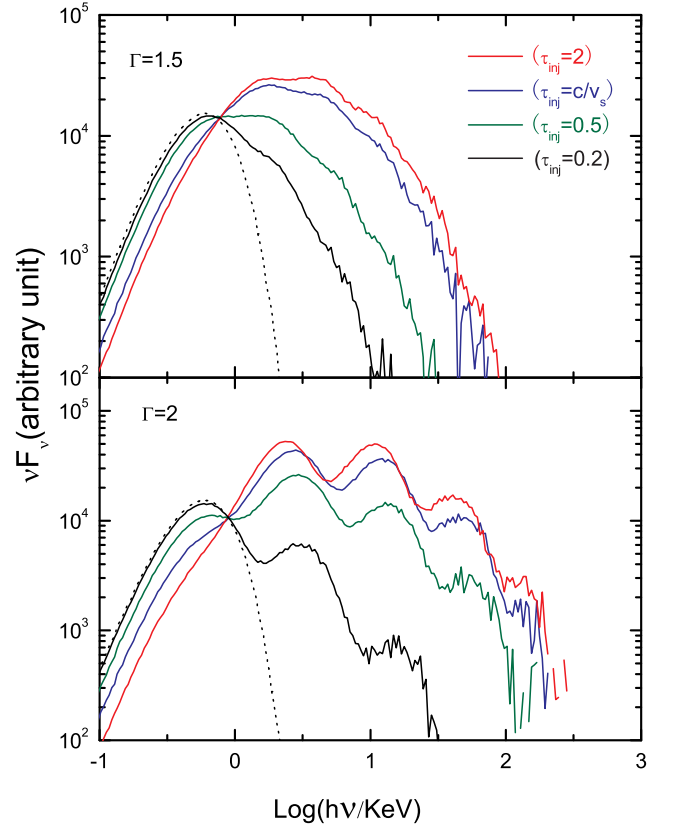


FIG. 1.— The time-integrated energy distribution of the escaping photons.  $10^6$  photons, with a black body distribution at  $k_B T_{th} = 0.15$  KeV (black dotted line), are injected at four different times, corresponding to optical depths of the pre-shocked medium of  $\tau_{\text{inj}} = 2, c/v_s, 0.5$  and  $0.2$ . The ejecta Lorentz factors are  $\Gamma = 1.5$  and  $\Gamma = 2$  for upper panel and lower panel respectively. Note, that the “humps” seen in the spectra are an artifact of the one-dimensional simulation, and are expected to be smoothed out in reality.

ues of  $\Gamma$  and  $\tau_{\text{inj}}$ . Note that the spectra are steeper (softer) at high energies, due to the longer time required for acceleration to higher energies, which implies a significant decrease in  $\tau$  during the acceleration process. The peak in  $\nu F_\nu$  is typically at few keV, and the spectrum is essentially cutoff beyond few hundred keV.

Fig. 2 shows the arrival time distribution of accelerated photons in different energy channels, for one single-time injection in a one-dimensional planar shock breakout, with particular values for  $\Gamma$  and  $\tau_{\text{inj}}$ . The higher energy photons (e.g.  $> 10$  keV, dashed lines) are delayed compared to the lower energy ones (e.g. 1-10 keV, solid lines of the same color). For the wind parameters chosen,  $\dot{M} = 10^{-4} M_\odot \text{yr}^{-1}$  and  $v_w = 10^8 \text{cm s}^{-1}$ , the delay is of order tens of seconds (for photons injected at the same  $\tau_{\text{inj}}$ ), and the decay time of the Compton flux is  $\sim 100$  s. Note that these curves are *not* the light curve. The light curve in this model would be produced by the convolution of the temporal profiles given in the figure with the temporal dependence of injected photon flux and energy. Thermal photons injected at different  $\Gamma$ ,  $\tau$  and different angles from the line of sight, depending on the anisotropic geometry of the radiation-dominated shock, will be continuously injected over a time much longer than the individual pulses seen in

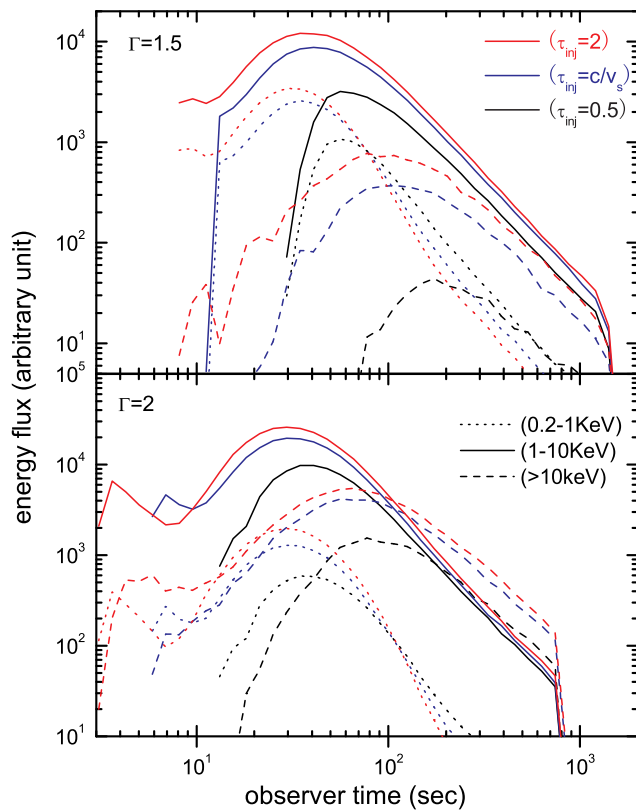


FIG. 2.— The temporal evolution of the flux of "accelerated photons" resulting from the injection of photons at a single given time, corresponding to a given value of  $\tau_{\text{inj}}$ , for a simplified planar shock breakout in one-dimension and two values of  $\Gamma$ . The wind parameters are:  $\dot{M} = 10^{-4} M_{\odot} \text{yr}^{-1}$  and  $v_w = 10^8 \text{cm s}^{-1}$ . The injected photon temperature is  $k_B T_{\text{th}} = 0.15 \text{KeV}$ . Note that these curves are *not* the light curve. The light curve in this model would be produced by a convolution of the temporal profiles given in the figure with the temporal dependence of the injected photon flux and energy, its total duration being of the same order as that of the light curve for the thermal photons,  $\sim 10^3$  s, in the case of GRB060218.

Fig. 2. In the following section, we apply these results to the case of GRB060218/SN2006aj.

### 2.3. GRB060218/SN2006aj

The spectral analysis of GRB060218 shows that the spectrum from X-ray to gamma-ray energies can be modelled as the sum of a thermal component plus a power-law with a high-energy cutoff (Campana et al. 2006; Liang et al. 2006) and that the non-thermal emission detected by Swift BAT and XRT is likely to be of the same origin (Liang et al. 2006). This is consistent with the theoretical expectations from the Comptonization model discussed above. In particular, the location of the  $\nu F_{\nu}$  peak at a few keV is consistent with X-ray flash nature of GRB060218. As pointed out by Dai et al (2006), the non-detection of an optical emission of the synchrotron tail of the nonthermal X-ray emission is an argument against the synchrotron internal shock origin for the nonthermal emission. This lack of nonthermal optical emission is naturally accounted for in our model, since repeated Compton scattering can only boost thermal photons to higher energies.

Since the characteristic evolution time of GRB060218 is

$\sim 1000$  s, the  $\sim 100$  s spread introduced by the repeated scattering in our model is unimportant. The  $\sim 1000$  s evolution timescale of the X-ray emission of GRB060218 has been argued to be dominated by light travel time effects, possibly enhanced by the lateral dynamic time of a non-spherical shock expansion (Campana et al. 2006; Waxman et al. 2007). As pointed out in Waxman et al. (2006), the mildly-relativistic ejecta in GRB060218/SN2006aj is likely to be anisotropic, either due to an anisotropic explosion, or due to being driven by a jet. This, together with an anisotropic wind profile caused by rotation (Meynet & Maeder 2007) should lead to significant departures from sphericity in the shock propagation. In an anisotropic shock, the timescale is no longer the spherical value  $r/c \sim 200$  s, but is rather given by the sideways pattern expansion timescale, which depends on the angular velocity profile of the anisotropic shell (e.g. at larger angles the shock emerges later due to a decreasing velocity profile or due to an increasing wind density away from the symmetry axis, etc.). In any case, the duration of the non-thermal part should be comparable to that of the thermal part, which is of the order of  $\sim 1000$  s. In this context, the temporal evolution of GRB060218 would reflect the fact that, at different times, we see radiation from different regions of the shock breakout that are characterized by different  $\Gamma$  and  $\tau$ . The light curve would be produced by the convolution of the temporal profiles given in the figure with the temporal dependence of injected photon flux and energy. We point out that a complete calculation of the light curve would require a knowledge of the intensity of the thermal photons at different times (corresponding to different  $\tau_{\text{inj}}$ ) and of their temperatures. In order to derive these quantities, a detailed calculation of the shock structure would be required, which is beyond the scope of the present paper.

### 3. DISCUSSION

We have discussed a model for the early gamma-ray and X-ray emission of low luminosity GRBs which are associated with supernovae, based on bulk Comptonization of thermal photons by a semi-relativistic ejecta. One expects the following basic characteristics for the gamma-ray bursts produced through the above mechanism:

1) Smooth light curve profiles. The production of the gamma-rays is through the repeated bulk-Compton scattering of thermal photons emitted by the radiation dominated shock. The light curve should follow the time behavior of the shock breakout and should therefore be smooth. The light curves would generally have a simple profile without multi-peak structure. The three nearby low-luminosity bursts, GRB060218, GRB980425 and GRB031203, all have smooth light curves, consistent with this picture. Given that GRB980425 and GRB031203 are also believed to have produced mildly relativistic ejecta, it is possible that the gamma-ray emission is due to supernova shock breakout also in these two bursts. Based on the association between GRB980425 and SN1998bw, Bloom et al. (1998) speculated that there may exist a subclass of smooth light curve GRBs produced by SNe. The duration of GRB980425 and GRB031203 is only tens of seconds, which can be interpreted as due to shock breakout from the progenitor envelope, implying that the wind surrounding the progenitor is optically thin. The characteristic variability time of GRB980425 and GRB031203 is a few seconds, corresponding to  $R(\tau = 1) \sim 10^{11} \text{cm}$ , which is comparable to the stellar radius of a Wolf-Rayet star. The speculation that the stellar wind surrounding GRB980425 is optically thin is consistent with the wind mass-loss rate inferred from the X-

ray and radio afterglow of GRB980425/SN1998bw (Waxman 2004; Li & Chevalier 1999). The longer timescale of GRB 060218 can, on the other hand, be interpreted in terms of the shock breaking out from an optically thick wind.

2) The spectrum is expected to be composed of a simple power-law, with a high energy cutoff lower than few  $\times 100$  keV, and a thermal X-ray component. The spectrum of the gamma-ray emission can be modelled as a cutoff power law rather than the Band function for the usual bursts. The spectrum is expected to evolve from hard to soft since the spectral index becomes smaller and the cutoff energy decreases as the optical depth decreases. The spectra of three nearby SN-GRBs, indicated in Table 1, are consistent with this cutoff power-law spectrum.

Cosmological GRBs with isotropic equivalent energies  $E \sim 10^{51} - 10^{54}$  erg are generally believed to be produced through internal shocks in relativistic jets with Lorentz factor  $\Gamma \gtrsim 100$  (for a recent review, see Mészáros 2006). In the collapsar scenario, relativistic jets can break free from the star along the rotation axis of a collapsing stellar core, provided that the central engine feeding time of the jets is sufficient long. Light curve breaks in the afterglow emission attributed to jet effects have been seen in many bursts. On the other hand, three nearby GRBs, GRB980425/SN1998bw, GRB031203/SN2003lw and GRB060218/SN2006aj, have isotropic energies in the range  $\sim 10^{48} - 10^{49}$  erg, much lower than typical cosmological bursts. Due to their proximity, the inferred intrinsic rate of these sub-energetic events is, however, much higher (Soderberg et al. 2006; Liang et al. 2006b), raising difficulties in interpreting these events as typical GRBs observed off-axis (Cobb et al. 2006). Both the properties of the prompt gamma-ray emission and of the afterglows are different from those of typical cosmological bursts. Up to now there is no straightforward evidence for the presence of highly relativistic jets in these sub-energetic bursts, but instead, there does exist evidence for mildly relativistic ejecta in these bursts. Thus, it could be that the relativistic jets in these events are much weaker, giving most of their energy to

the outer slow material when they are burrowing their way through the star, which leads to a much wider anisotropic pattern of outflow. This could be the case even if the jets are choked before emerging outside the stellar envelope, due e.g. to an insufficient central engine feeding time. Whether there is a relativistic jet or not can be probed through sub-GeV to GeV observations during the shock breakout (Wang & Mészáros 2006)

Mildly relativistic ejecta may also exist in the usual high-luminosity long GRBs, since shock acceleration is expected to accompany the supernova. This might explain the low-velocity component, other than the relativistic jet, found by Berger et al. (2003) and Kartik et al. (2003) in another nearby supernova-connected GRB, namely GRB030329/SN2003dh, from the radio and optical afterglow more than 1.5 days after the explosion. In this burst, the gamma-ray emission from the mildly relativistic ejecta is lower than that of the relativistic jet, since the latter has a much higher isotropic energy. As suggested by Berger et al (2003), the total energy in the low velocity component and the relativistic jet may be a roughly constant quantity, the only variable being the ratio of these two components. In this vein, we would predict that at high redshifts there could be many GRB/SN with stronger lower velocity and weaker relativistic jet components, which would be harder to detect, even though their rates of occurrence might exceed that of the more easily detectable bursts with weak low-velocity and stronger relativistic jets.

We would like to thank S. Campana, Z. G. Dai, B. Zhang, E. W. Liang and Nino Panagia for useful discussions. This work is partially supported by NASA NAG5-13286, NSF AST 0307376, the National Natural Science Foundation of China under grants 10403002, 10221001 and 10473010, and the Foundation for the Authors of National Excellent Doctoral Dissertations of China (for XYW). ZL & EW are partially supported by ISF and AEC grants.

#### REFERENCES

- Berger, E., et al., 2003, *Nature*, 426, 154  
 Blandford, R. D. & Eichler, D. 1987, *Phys. Rep.* 154, 1  
 Blandford, R. D. & Payne, D. G., 1981, *MNRAS*, 194, 1041  
 Blinnikov, S. I., Eastman, R., Bartunov, O. S., Popolitov, V. A., & Woosley, S. E. 1998, *ApJ*, 496, 454  
 Bloom, J. S., Kulkarni, S. R., Harrison, et al., *ApJ*, 506, L105  
 Campana, S. et al. 2006, *Nature*, 442, 1008  
 Chevalier, R. A. & Li, Z.-Y. 1999, *ApJ*, 520, L29  
 Cobb, B. E. et al., 2006, *ApJ*, 645, L113  
 Colgate, S. A. 1974, *ApJ*, 187, 333  
 Dai, Z. G., Zhang, B., & Liang, E. W., *astro-ph/0604510*  
 Dermer, C. D.; Liang, E. P., & Canfield, E., 1991, *ApJ*, 369, 410  
 Ensmann, L. & Burrows, A., 1992, *ApJ*, 393, 742  
 Fan, Y., Piran, T. & Xu, D. 2006, 2006, *JCAP*, 9, 13  
 Felli & Panagia 1982, *ApJ*, 262, 650  
 Ghisellini, G. et al., 2006a, *MNRAS*, 372, 1699  
 Ghisellini, G. et al., 2006b, *MNRAS*, 375, L36  
 Gorosabel, J. et al., 2006, *A&A*, 459, L33  
 Gruzinov, A. & Mészáros, P., 2000, *ApJ*, 539, L21  
 Kaneko, Y. et al. 2006, *ApJ*, accepted, *astro-ph/0607110*  
 Klein, R. I. & Chevalier, R. A. 1978, *ApJ*, 223, L109  
 Krall, N. & Trivelpiece, A., *Principles of Plasma Physics* (McGraw-Hill, New York, 1973).  
 Kulkarni, S. R. et al. 1998, *Nature*, 395, 663.  
 Li, L.-X. 2007, *MNRAS*, 375, 240  
 Li, Z.-Y. & Chevalier, R.A. 1999, 526, 716  
 Liang, E. W. et al. 2006a, *astro-ph/0606565*  
 Liang, E. W. Zhang, B., & Dai, Z. G. 2006a, *subm. ApJ*, *astro-ph/0605200*  
 Liang, E. W., Zhang, B. B., Stamatikos, M. et al. 2006, *ApJ*, 653, L81  
 Matzner, C. D., & McKee, C. F. 1999, *ApJ*, 510, 379  
 Mazzali, P. A. et al. 2006, *Nature*, 442, 1018  
 Mészáros, P. & Rees, M. J. 2001, *ApJ*, 556, L37  
 Mészáros, P., 2006, *Rep. Prog. Phys.*, 69, 2259  
 Meynet, G. & Maeder, A., 2007, *astro-ph/0701494*  
 Mirabel, N. et al. 2006, 643, L99  
 Modjaz, M. et al. 2006, *ApJ*, 645, L21  
 Nugis, T. & Lamers, H. J. G. L. M. 2000, *A&A* 360, 227  
 Nugis, T. & Lamers, H. J. G. L. M. 2002, *A&A* 389, 162  
 Pian, E. et al. 2006, *Nature*, 442, 1011  
 Pozdniakov, L. A., Sobol, I. M. & Syunyaev, R. A. 1976, *Soviet Astronomy Letters*, 2, 55  
 Pozdniakov, L. A., Sobol, I. M. & Syunyaev, R. A. 1983, *Astrophys. Space Phys. Rev.*, 2, 189  
 Ramirez-Ruiz, E., Celotti, A. & Rees, M. J., 2002, *MNRAS*, 337, 1349  
 Sazonov, S. Y., Lutovinov, A. A. & Syunyaev, R. A., 2004, *Nature*, 430, 646  
 Shrader, C. & Titarchuk, L. 1998, *ApJ*, 499, L31  
 Soderberg, A. et al. 2006, *Nature*, 442, 1014  
 Sollerman, J. et al. 2006, *A&A*, 454, 503  
 Tan, J. C., Matzner, C. D. & McKee, C., 2001, *ApJ*, 551, 946  
 Thompson, C. 1994, *MNRAS*, 270, 480  
 Titarchuk, L. & Shrader, C. 2005, *ApJ*, 623, 362  
 Wang, X. Y., & Mészáros, P. 2006, *ApJ*, 643, L95  
 Watson, D. et al. 2004, *ApJ*, 605, L101  
 Waxman, E. & Loeb, A., 1999, *ApJ*, 515, 721  
 Waxman, E. & Loeb, A., 2001, *Phys. Rev. Lett.*, 87, 071101  
 Waxman, E. 2004, *ApJ*, 605, L97

TABLE 1  
THE SPECTRUM OF THREE NEARBY LOW-LUMINOSITY GRBS

GRB/SN	$z$	$E_{\gamma,iso}(\text{erg})$	$\alpha$	$\varepsilon_c(\text{KeV})$	references*
GRB980425/SN1998bw	0.0085	$(8.5 \pm 0.1) \times 10^{47}$	$0.45 \pm 0.22$	$\sim 200$	1;3
GRB031203/SN2003lw	0.105	$(4 \pm 1) \times 10^{49}$	$0.63 \pm 0.06$	$> 190$	2;4
GRB060218/SN2006aj	0.0331	$(6.2 \pm 0.3) \times 10^{49}$	0.45	$\sim 30^{\S}$	1;3;5; 6

\*The redshift  $z$ , spectral index  $\alpha$  ( $F_{\nu} \propto \nu^{-\alpha}$ ) and cutoff energy  $\varepsilon_c$  of the three nearby, sub-luminous SN-connected GRBs. References: (1) Ghisellini et al. (2006); (2) Sazonov et al. 2004; (3) Kaneko et al. 2006; (4) Sazonov et al. 2004; (5) Campana et al. 2006; (6) S. Campana, private communication.

$\S$  For the time  $< 300$  seconds after the trigger.

Waxman, E., Mészáros, P. & Campana, S. 2007, astro-ph/0702450

Weaver, T. A. 1976, ApJS 32, 233

Zhang, W. Q., Woosley, S. E. & MacFadyen, A. I., 2003, ApJ, 586, 356